Dyes and Pigments 85 (2010) 51–56

Contents lists available at ScienceDirect

Dyes and Pigments

journal homepage: www.elsevier.com/locate/dyepig

The photo- and electrochemical properties and electronic structures of conjugated diphenylanthrazolines

Shan Liu [a,b], Qiang Wang [c], Peng Jiang [a], Rui Liu [a], Guangliang Song [a], Hongjun Zhu [a,*], Shuo-Wang Yang [d,**]

[a] Department of Applied Chemistry, College of Science, Nanjing University of Technology, Nanjing 210009, PR China
[b] Chemical Engineering Department, Nanjing College of Chemical Technology, Nanjing 210048, PR China
[c] School of Chemical and Biomedical Engineering, Nanyang Technological University, 62 Nanyang Drive, Singapore 637459, Singapore
[d] Institute of High Performance Computing, 1 Fusionopolis Way, #16-16 Connexis, Singapore 138632, Singapore

ARTICLE INFO

Article history:
Received 20 August 2009
Received in revised form
2 October 2009
Accepted 2 October 2009
Available online 22 October 2009

Keywords:
Diphenylanthrazoline
Fluorescence
Optical property
Optoelectronic materials
Electrochemical property
Organic light-emitting diodes (OLED)

ABSTRACT

The effect of molecular structure on the photophysical, electronic structure properties of a series of 9 conjugated diphenylanthrazolines were explored by UV–vis adsorption, photoluminescence spectroscopy, cyclic voltammetry and quantum chemical calculations. The featureless adsorption bands observed (λ^{Abs}_{max}: 382–420 nm) revealed low optical band gaps (2.05–2.25 eV) and the photoluminescence emission spectra (λ^{Em}_{max}: 480–546 nm) and large Stokes shift (78–148 nm) suggested the presence of excimers in the solid state. With only one exception, the diphenylanthrazolines displayed reversible electrochemical reduction with potentials of −1.03 to −1.40 V, low ionization potentials (~5.91–6.29 eV), relative to that of a saturated calomel electrode and high electron affinity (~3.44–3.59 eV). Quantum chemical calculations using DFT B3LYP/6-31G showed nearly identical LUMO (−2.2 ~ −2.3 eV) and HOMO (−5.2 ~ −5.6 eV) values, revealing that both the electronic properties and the geometries of the diphenylanthrazolines depended on the anthrazoline backbone.

1. Introduction

Conjugated π-electron materials are of immense interest as a consequence of their wide variety of semiconducting and conducting properties and enjoy widespread usage in organic light-emitting diodes (OLED) [1–7], photovoltaics [8–14], field-effect transistors [15–21] and other aspects of "plastic electronics" [22]. Among these materials, conjugated polyanthrazolines have been extensively investigated as n-type (electron-transport) organic semiconductors over the past 20 or so years [23–34]. Surprisingly, investigations on synthesis, photophysical and electrochemical properties of small molecules which may serve as structurally well-defined model systems for the corresponding polyanthrazolines are limited. However, in 2003, five diphenylanthrazoline derivatives were reported by Jenekhe [6] who showed that these small molecules had high electron affinity and high thermal stability and were promising electron-transport materials for OLED. Then in 2008, a theoretical study concerning molecular structure and substitution effects on diphenylanthrazolines was demonstrated by Glossman-Mitnik [34] who showed that diphenylanthrazolines had good HOMO-LUMO ratio and were potential n-type organic semiconductors. In this context, the development of new anthrazoline molecules and the further study of the underlying structure–property relationships presented an interesting challenge.

Recently, a series of thermally stable diphenylanthrazolines (**1a**–**1i**, Fig. 1) reported by our group [35] show the lowest energy absorption bands (λ^{Abs}_{max}: 394–433 nm) from π–π* transitions, revealing low optical band gaps (2.59–2.80 eV). And they emit blue fluorescence with emitting maxima (λ^{Em}_{max}) ranging from 430 to 466 nm in diluted toluene solution. The results suggest that these compounds have a potential application as electron-transporting electroluminescent materials, which motivated us to further investigate the properties of these diphenylanthrazolines. In this paper, photophysical and electrochemical properties of this series of diphenylanthrazolines in the solid state were studied. Quantum chemical calculations were also performed to gain insight into the electronic properties and the geometries of these compounds.

* Corresponding author. Tel./fax: +86 25 83172358.
** Corresponding author. Tel.: +65 64191343; fax: +65 67780522.
E-mail addresses: zhuhjnjut@hotmail.com (H. Zhu), yangsw@ihpc.a-star.edu.sg (S.-W. Yang).

0143-7208/$ – see front matter © 2009 Elsevier Ltd. All rights reserved.
doi:10.1016/j.dyepig.2009.10.003

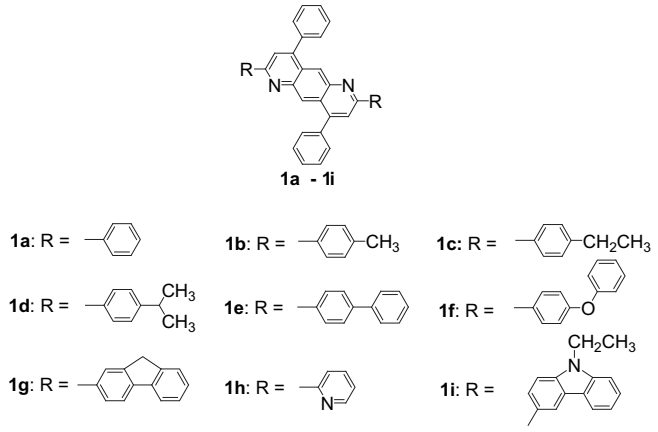

Fig. 1. Molecular structures of **1a**–**1i**.

2. Experimental section

2.1. Materials

The detailed synthesis, purification, and characterization of the diphenylanthrazolines **1a**–**1i** are described elsewhere [35]; the compounds were characterized for their structures and other physical properties.

Acetonitrile and chloroform (Shanghai Lingfeng Chemical Company) were purified by redistillation. Tetra-n-butylammonium perchlorate (TBAP) (Quzhou Guomao Chemical Co., Ltd) and ferrocene (Sinopharm Chemical Reagent Co., Ltd) were purified by recrystallization twice from ethanol. All other reagents were obtained from Sinopharm Chemical Reagent Co., Ltd and used as received.

2.2. Measurements

2.2.1. Photophysics

Optical absorption spectra were obtained by using an HP-8453 UV/vis/near-IR Spectrophotometer (Agilent). Photoluminescence spectra were carried out on an LS-55 spectrophotometer (Perkin–Elmer).

2.2.2. Cyclic voltammetry

For cyclic voltammetry, an electrolyte solution of 0.1 M TBAP in acetonitrile and chloroform (V/V = 7:3) was used in all experiments. All solutions in the cell were purged with ultrahigh-purity N_2 for 10–15 min before each experiment, and a blanket of N_2 was used during the experiment. Platinum wire electrodes were used as both counter and working electrodes and silver/silver ion (Ag in 0.1 M $AgNO_3$ solution, from CHI, Inc.) was used as a reference electrode. The Ag/Ag^+ ($AgNO_3$) reference electrode was calibrated at the beginning of the experiments by running cyclic voltammetry on ferrocene as the internal standard in an identical cell without any diphenylanthrazoline on the working electrode. The potential values obtained in reference to Ag/Ag^+ electrode were converted in reference to internal standard of ferrocenium/ferrocene (Fc^+/Fc). The diphenylanthrazolines were coated onto the working electrode by dipping the Pt wire electrode in the diphenylanthrazolines solutions. The diphenylanthrazolines solutions were made in 1–2 wt % formic acid/chloroform. The coated electrode was dried in a vacuum oven at 80 °C resulting in a thin film of diphenylanthrazoline - formic acid complex on the Pt electrode. To obtain the pure diphenylanthrazoline coatings on the electrode, the electrode-bound diphenylanthrazoline - formic acid complex was electrochemically converted to the pure diphenylanthrazoline before proceeding with the reduction or oxidation cycles by a method reported in literature [31]. The electrochemical equipment used for the experiments was a CHI600c Electrochemical Workstation. Data were collected and analyzed using Electrochemical Analysis System Software for CHI600c on PC computer. A scan rate of 40 mV/s was used in obtaining all the cyclic voltammograms (CVs) reported here.

The potential values obtained versus Fc^+/Fc were converted to versus saturated calomel electrode (SCE) by adding a constant of 0.1588 V to them. The solid-state ionization potential (IP) and electron affinity (EA) of the diphenylanthrazolines were estimated by using following relations: $[E_{onset}]^{ox} = IP-4.4$ and $[E_{onset}]^{red} = EA-4.4$, where $[E_{onset}]^{ox}$ and $[E_{onset}]^{red}$ are the onset potentials for the oxidation and reduction of diphenylanthrazolines versus SCE. The onset potentials were determined from the intersection of two tangents drawn at the rising current and background charging current of a cyclic voltammogram [31].

2.2.3. Theory and computational details

Computations were performed using the Gaussian 03 simulation program [36] through the use of DFT based on Kohn-Sham approximations [37]. This method can determine molecular properties as a function of electronic density when the molecules are in their ground state. Gaussian 03 has several functional options and basis sets which are available in its DFT module.

The equilibrium geometry for each of the nine neutral molecules was found by using the hybrid B3LYP functional, which is a hybrid HF-DFT functional that combines Becke's three parameter exchange functional [38] with Lee–Yang–Parr's correlation functional [39]. 6-31G basis set was also used. Equilibrium geometry was then calculated by using these sets.

3. Results and discussion

3.1. Photophysical properties

Comparisons of **1a**–**1i** in UV and visible light in THF solution are shown in Fig. 2.

The solution of **1a**–**1h** appears to be colorless in visible light and emits blue fluorescence in UV light (band 254 nm), while the solution of **1i** appears to be yellow-green in visible light and emits strong green fluorescence in UV light.

The solid-state optical absorption spectra of compounds **1a**–**1i** are shown in Fig. 3. In addition to their broad featureless characteristics, these solid state absorption bands are significantly red shifted from the dilute solution ones [6] for **1a**–**1f** and blue shifted for **1g**–**1i**. The 1–24 nm red shifts in absorption maximum for **1a**–**1f** suggest there is a slight increase in conjugation length in the solid state. Such an increase in conjugation length in the solid state is expected from the more planar conformations due to the π-stacking in the solid state which was observed in the X-ray single-crystal structures of some other diphenylanthrazoline derivatives reported in literature [6]. As for **1g**–**1i**, the 12–15 nm blue shifts are probably due to a decrease in conjugation length in the solid state. Optical band gaps (E_g^{opt}) determined from the absorption edge of the solid-state spectra are given in Table 1. The optical band gap varies from 2.05 eV in **1i** to 2.25 eV in **1g** and **1h**.

The PL emission spectra of **1a**–**1i** in the solid state are shown in Fig. 4. The structured PL emission bands in solution [6] are also seen in the solid state. All nine compounds have structured emission bands with the emission maximum ranging from 480 nm for **1g** to 546 nm for **1e** and the large Stoke shifts ranging from 78 nm for **1g** to 148 nm for **1h**. The similarities of the emission spectral features in conjunction with the π-stacking of the molecules in the solid state suggest that excimer emission [3,6,40] best describes the solid-state luminescence of **1a**–**1i**.

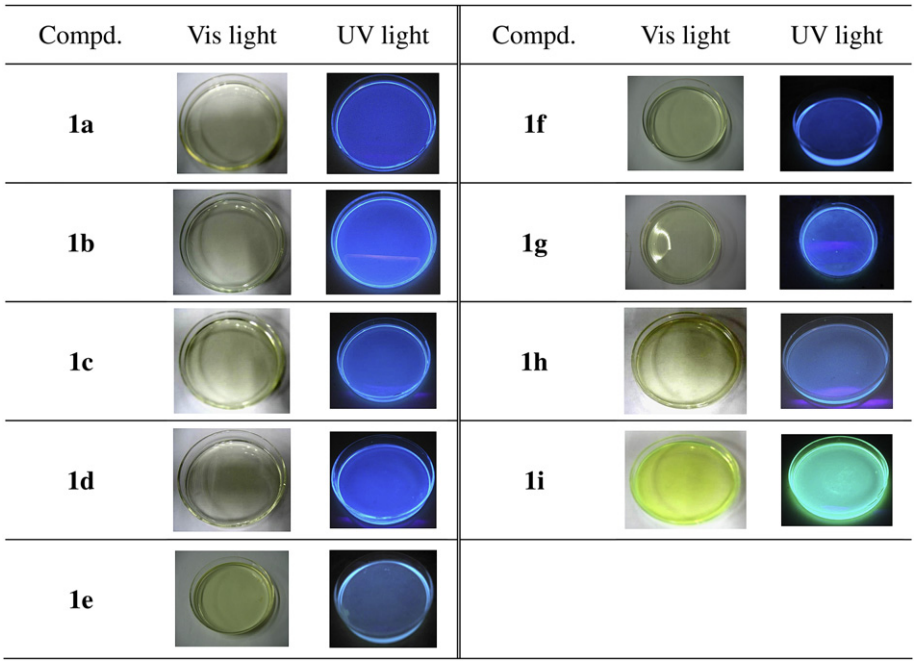

Fig. 2. Color comparison of **1a**–**1i** in UV and visible light in THF($c = 5.0 \times 10^{-5}$ M).

3.2. Electrochemical properties

Cyclic voltammetry was done on thin films of all diphenylanthrazolines **1a**–**1i**. The cyclic voltammograms (CVs) of these nine molecules are shown in Fig. 5. Quasi-reversible reduction peaks were seen in CVs of **1b**–**1i**. But in CV of **1a**, a quasi-reversible reduction peak was not observed as the reduced molecule becomes soluble in the electrolyte [6]. Molecules **1b**, **1e**, **1f** had one irreversible oxidation peak, which is in good agreement with other compounds containing diphenylanthrazoline backbones reported in literature [6]. In the case of **1a**, **1c**, **1d**, **1g**, **1h**, **1i**, the irreversible oxidation peak was not seen when scanned to 2.0 V.

Table 2 shows the solid-state electrochemical data for **1a**–**1i**. HOMO and LUMO levels were estimated from the onset potentials by comparison to ferrocene (4.4 eV versus vacuum) [6,31,41,42]. Electron affinities (LUMO) were estimated from the onset of the reduction wave (EA = E_{red}^{onset} + 4.4). The EA value of compound **1a** has been reported in the literature [6] as 3.10 eV (versus SCE), which is different from our result (3.44 eV, versus SCE). The origin for this difference is not clear due to the differences of electrolyte and solvent systems. All nine diphenylanthrazolines have electron affinities between 3.44 and 3.59 eV (below vacuum), revealing the promising electron-transport properties (n-type) for OLEDs. The reduction potentials of all the molecules are relatively unchanged by the substituent (R groups), indicating that the LUMOs lie on the anthrazoline moiety. Even the electron-rich carbazole substituted molecule (**1i**), which as expected has the lowest oxidation potential, has essentially the same LUMO level as the other molecules.

The formal reduction potential (E_{red}^{onset}) varies from −1. 03 V (vs SCE) for **1g** to −1.40 V for **1h** (Table 2). The estimated ionization potential (IP = E_{ox}^{onset} + 4.4 eV) is reduced from 6.29 eV in **1f** to 5.91 eV in **1i**. Also shown in Table 2 are the electrochemically derived band gap (E_g^{el}) of thin films of the diphenylanthrazolines. The E_g^{el} varies from 2.35 eV for **1i** to 2.71 eV for **1f**. The electrochemical band gap is smallest in **1i** as expected from the large delocalization length facilitated by the substituted groups of N-ethyl carbazole. The measured electrochemical band gap of each diphenylanthrazoline is higher than the corresponding optical

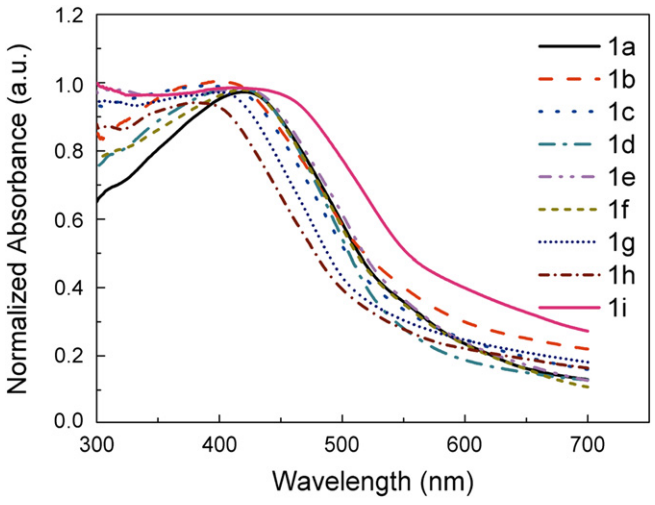

Fig. 3. Optical absorption spectra of **1a**–**1i** in the solid state.

Table 1
Spectra properties of **1a**–**1i**.

Compd.	$\lambda^{Abs}{}_{max}$[a] solution (nm)	$\lambda^{Em}{}_{max}$[a] solution (nm)	$\lambda^{Abs}{}_{max}$ solid (nm)	$\lambda^{Em}{}_{max}$ solid (nm)	Stokes shift solid (nm)	E_g^{opt} solid(eV)
1a	396	430	420	535	115	2.08
1b	401	431	403	533	130	2.12
1c	401	431	402	528	126	2.13
1d	401	432	415	537	122	2.14
1e	408	438	419	546	127	2.09
1f	410	439	419	537	118	2.10
1g	417	445	402	480	78	2.25
1h	394	433	382	530	148	2.25
1i	433	466	416	524	108	2.05

[a] Data in toluene solution were quoted from literature [6].

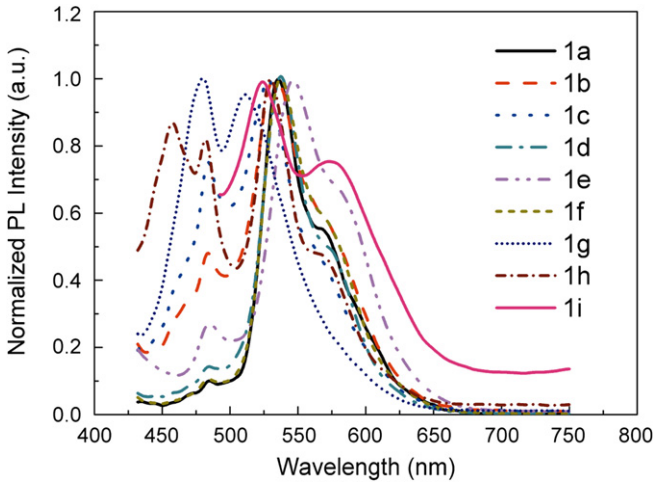

Fig. 4. PL spectra of **1a**–**1i** in the solid state.

band gap (E_g^{opt}), which can be negligible because the experimental results as well as the theoretical calculations in the following section are qualitatively correct in explaining the doping characteristics of these diphenylanthrazolines which are clearly better n-type materials than p-type. Such differences between E_g^{el} and E_g^{opt} have also been discussed in the literature [31,43].

Table 2
Electrochemical Properties of thin films of **1a**–**1i**[a].

Compd.	E_{red}^{peak} (V)	E_{red}^{onset} (V)	EA[b] (eV)	E_{ox}^{peak} (V)	E_{ox}^{onset} (V)	IP[b] (eV)	E_g^{el} [b] s(eV)
1a	−1.30	−0.96	3.44	———[c]	1.65	6.05	2.61
1b	−1.22	−0.86	3.54	1.96	1.75	6.15	2.61
1c	−1.35	−0.87	3.53	———[c]	1.66	6.06	2.53
1d	−1.13	−0.86	3.54	———[c]	1.72	6.12	2.58
1e	−1.19	−0.95	3.45	1.96	1.75	6.15	2.70
1f	−1.04	−0.82	3.58	2.04	1.89	6.29	2.71
1g	−1.03	−0.81	3.59	———[c]	1.57	5.97	2.38
1h	−1.40	−0.84	3.56	———[c]	1.56	5.96	2.40
1i	−1.16	−0.84	3.56	———[c]	1.51	5.91	2.35

[a] All potentials vs SCE reference.
[b] EA (LUMO) = E_{red}^{onset} + 4.4 eV; IP (HOMO) = E_{ox}^{onset} + 4.4 eV; E_g^{el} = IP − EA.
[c] The irreversible oxidation peak was not seen when scanned to 2.0 V.

3.3. Theoretical calculation

To gain insight into the electronic properties and the geometries of the diphenylanthrazolines, quantum chemical calculations were performed. In the calculations, the ground state geometries of **1a**–**1i** were fully optimized using density functional theory (DFT) at the B3LYP/6-31G level, as implemented in Gaussian 03. DFT/B3LYP calculation of lowest excitation energies was performed at the optimized geometries of the ground states. The optimized structures of all the compounds (**1i** as an example, Fig. 6) reveal that the substituted moieties attached to both ends of the molecule are nearly coplanar with the anthrazoline backbone. Therefore, π-electron

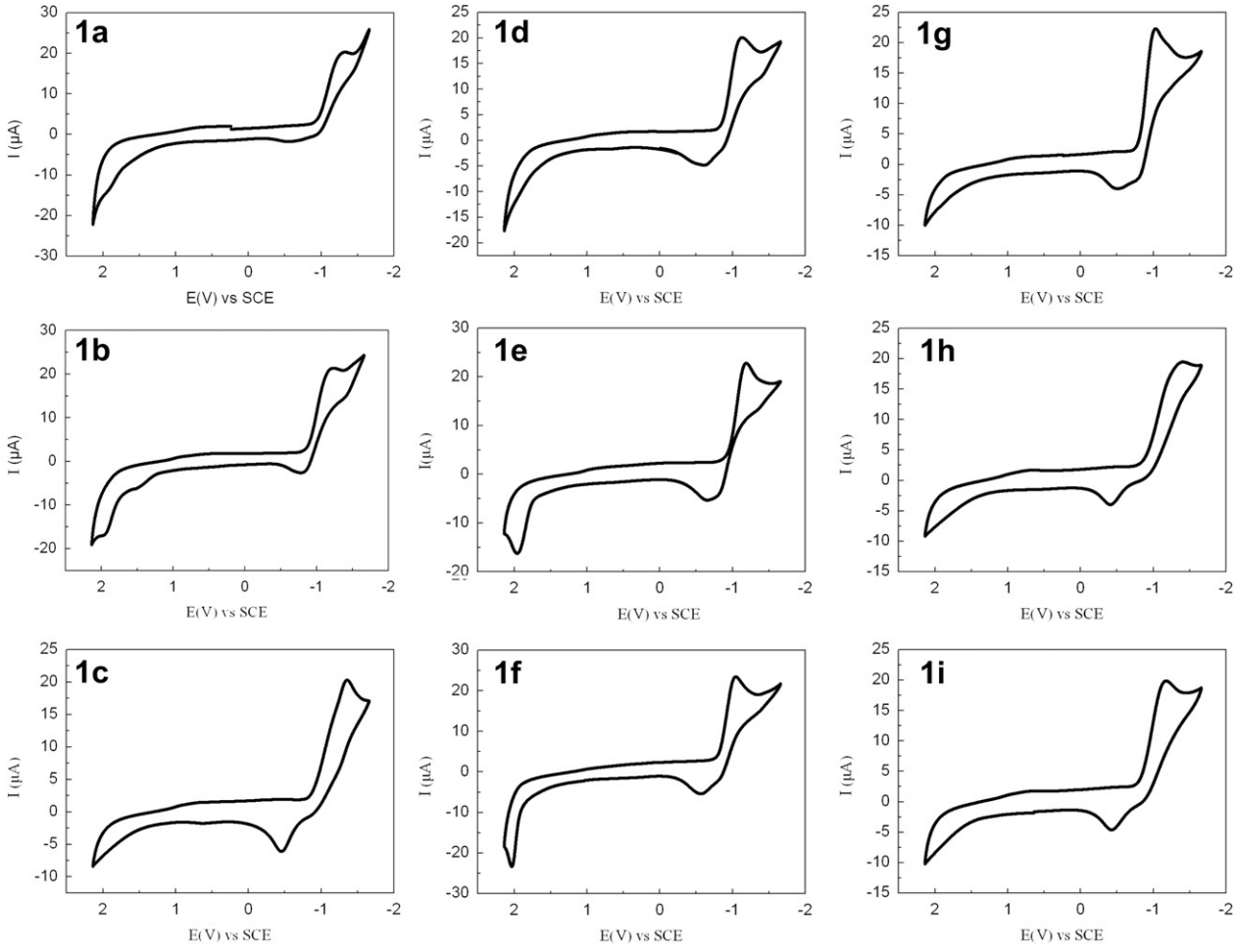

Fig. 5. Cyclic voltammograms of thin films of **1a**–**1i** coated on a Pt wire electrode. Scan rate = 40 mV/s.

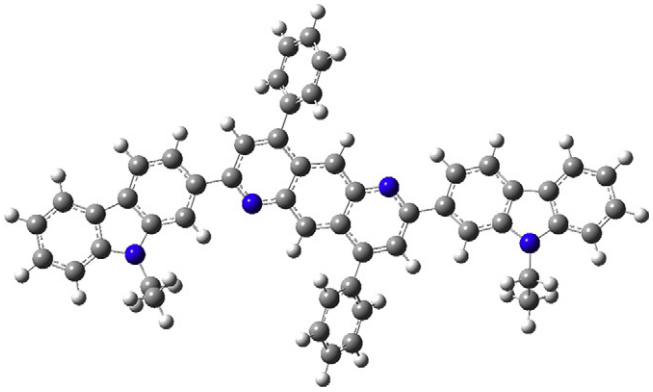

Fig. 6. B3LYP/6-31G optimized geometry of compound **1i**.

delocalization between those units is unlikely to be negligible. In their HOMO orbitals (Fig. 7), the π-electrons are able to delocalize over the entire anthrazoline backbone and end-capped moieties. In all cases, the HOMO is delocalized extensively over the whole π-conjugated systems via the anthrazoline chain and the terminal substituents, while the LUMO is delocalized only through the anthrazoline chain units as illustrated in Fig. 7. Therefore, a significant change in charge distribution would result upon the HOMO - LUMO transition in the compounds **1a**–**1i**. The HOMO - LUMO energy differences (energy band gaps, calculated E_g^{cal}) at DFT/B3LYP level of theory are presented in Table 3. The result indicates that E_g^{cal} values decrease as the electron-donating ability of end-capped moieties and the length of π-conjugated system increase. These predicted E_g^{cal} values are much higher than those estimated from the onset of UV–vis absorption (E_g^{opt}) and the cyclic voltammograms (E_g^{el}). There are factors which may be responsible for the errors because the

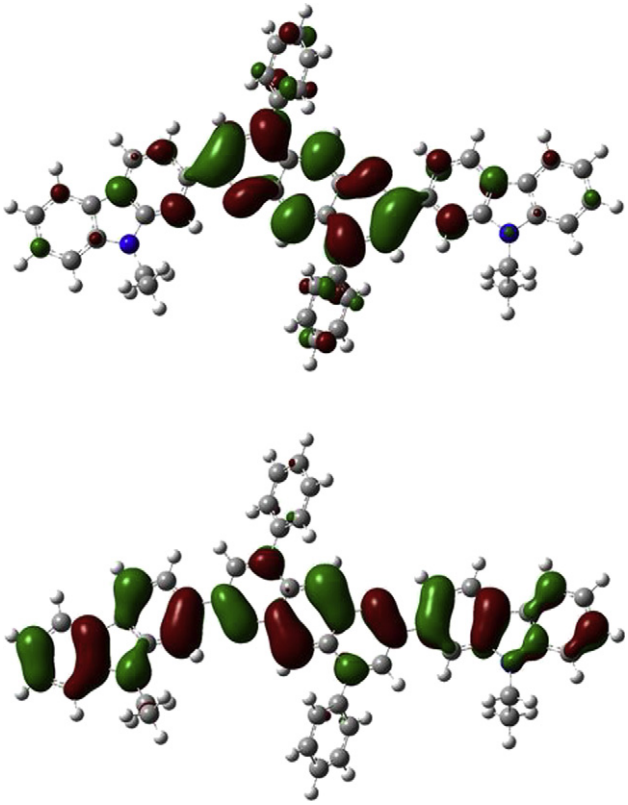

Fig. 7. HOMO (bottom) and LUMO (top) for molecules **1i** in gas phase.

Table 3
Energy values theoretically calculated for molecules **1a**–**1i** in gas phase.

Molecule	Energy (eV)		
	LUMO	HOMO	E_g^{cal}
1a	−2.247	−5.513	3.266
1b	−2.169	−5.402	3.233
1c	−2.173	−5.413	3.240
1d	−2.180	−5.401	3.221
1e	−2.283	−5.425	3.142
1f	−2.225	−5.381	3.156
1g	−2.240	−5.304	3.064
1h	−2.315	−5.575	3.260
1i	−2.196	−5.231	3.034

cal: Energies theoretically calculated for gas phase by means of DFT B3LYP/6-31G.

orbital energy difference between HOMO and LUMO is still an approximate estimation to the transition energy since the transition energy also contains significant contributions from some two-electron integrals. The real situation is that an accurate description of the lowest singlet excited state requires a linear combination of a number of excited configurations.

4. Conclusions

A series of nine diphenylanthrazoline derivatives have been investigated by Uv-vis adsorption spectrometry, photoluminescence emission spectrometry and cyclic voltammetry respectively, in order to explore the optical and electrochemical properties of π-conjugated anthrazolines in the solid state. The broad featureless Uv-vis adsorption spectra ($\lambda^{Abs}{}_{max}$: 382–420 nm) with red shifts from the dilute solution ones for **1a**–**1f** indicated there was a slight increase in conjugation length due to the π-stacking in the solid state. The PL emission spectra ($\lambda^{Em}{}_{max}$: 480–546 nm) with large Stokes shifts (78–148 nm) suggested there were excimers in the solid state. The investigation on electrochemical properties showed that ionization potential (IP, 5.91–6.29 eV) and electron affinity (EA, 3.44–3.59 eV) of these compounds were correlated with the main structural features of anthrazolines. Quantum chemical calculations by means of DFT B3LYP/6-31G indicated that **1a**–**1i** had nearly identical LUMO (−2.2 ∼ −2.3 eV) and HOMO (−5.2 ∼ −5.6 eV), which demonstrated the electronic properties and the geometries of the diphenylanthrazolines were mainly dependent on the anthrazoline backbone. Of the nine compounds, **1i** showed the lowest E_g^{opt} (2.1 eV), E_g^{el} (2.4 eV), and E_g^{cal} (3.0 eV) with $\lambda^{Em}{}_{max} = 524$ nm and is expected to be applicable as an electron-transporting (n-type) electroluminescent material. Further researches on compound **1i** in the application of OLED will be carried out and reported soon. We hope that this series of diphenylanthrazolines may also serve as model systems for investigating structure-property relationships with respect to the electronic, electrochemical, photoconductive, and nonlinear optical properties of π-conjugated polymers.

Acknowledgment

This work was supported in part by the postgraduate innovation fund of Jiangsu province (2007), P. R. China.

References

[1] Tang CW, Vanslyke SA. Organic electroluminescent diodes. Applied Physics Letters 1987;51(12):913–5.
[2] Burroughes JH, Bradley DDC, Brown AR, Marks RN, Mackay K, Friend RH, et al. Light-emitting-diodes based on conjugated polymers. Nature 1990;347(6293):539–41.
[3] Jenekhe SA, Osaheni JA. Excimers and exciplexes of conjugated polymers. Science 1994;265(5173):765–8.

[4] Baldo MA, O'Brien DF, You Y, Shoustikov A, Sibley S, Thompson ME, et al. Highly efficient phosphorescent emission from organic electroluminescent devices. Nature 1998;395(6698):151–4.
[5] Ho PKH, Kim JS, Burroughes JH, Becker H, Li SFY, Brown TM, et al. Molecular-scale interface engineering for polymer light-emitting diodes. Nature 2000;404(6777):481–4.
[6] Tonzola CJ, Alam MM, Kaminsky W, Jenekhe SA. New n-type organic semiconductors: synthesis, single crystal structures, cyclic voltammetry, photophysics, electron transport, and electroluminescence of a series of diphenylanthrazolines. Journal of the American Chemical Society 2003;125(44):13548–58.
[7] Brunner K, van Dijken A, Borner H, Bastiaansen J, Kiggen NMM, Langeveld BMW. Carbazole compounds as host materials for triplet emitters in organic light-emitting diodes: tuning the homo level without influencing the triplet energy in small molecules. Journal of the American Chemical Society 2004;126(19):6035–42.
[8] Granstrom M, Petritsch K, Arias AC, Lux A, Andersson MR, Friend RH. Laminated fabrication of polymeric photovoltaic diodes. Nature 1998;395(6699):257–60.
[9] Shirota Y. Organic materials for electronic and optoelectronic devices. Journal of Materials Chemistry 2000;10(1):1–25.
[10] Peumans P, Yakimov A, Forrest SR. Small molecular weight organic thin-film photodetectors and solar cells. Journal of Applied Physics 2003;93(7):3693–723.
[11] Thompson BC, Kim YG, McCarley TD, Reynolds JR. Soluble narrow band gap and blue propylenedioxythiophene-cyanovinylene polymers as multifunctional materials for photovoltaic and electrochromic applications. Journal of the American Chemical Society 2006;128(39):12714–25.
[12] Blom PWM, Mihailetchi VD, Koster LJA, Markov DE. Device physics of polymer: fullerene bulk heterojunction solar cells. Advanced Materials 2007;19(12):1551–66.
[13] Chochos CL, Economopoulos SP, Deimede V, Gregoriou VG, Lloyd MT, Malliaras GG, et al. Synthesis of a soluble n-type cyano substituted polythiophene derivative: a potential electron acceptor in polymeric solar cells. Journal of Physical Chemistry C 2007;111(28):10732–40.
[14] Gunes S, Neugebauer H, Sariciftci NS. Conjugated polymer-based organic solar cells. Chemical Reviews 2007;107(4):1324–38.
[15] Wang SJ, Oldham WJ, Hudack RA, Bazan GC. Synthesis, morphology, and optical properties of tetrahedral oligo(phenylenevinylene) materials. Journal of the American Chemical Society 2000;122(24):5695–709.
[16] Cornil J, Beljonne D, Calbert JP, Bredas JL. Interchain interactions in organic pi-conjugated materials: impact on electronic structure, optical response, and charge transport. Advanced Materials 2001;13(14):1053–67.
[17] Dimitrakopoulos CD, Malenfant PRL. Organic thin film transistors for large area electronics. Advanced Materials 2002;14(2):99–117.
[18] Facchetti A, Mushrush M, Yoon MH, Hutchison GR, Ratner MA, Marks TJ. Building blocks for n-type molecular and polymeric electronics. Perfluoroalkyl- versus alkyl-functionalized oligothiophenes (nT; n = 2–6). Systematics of thin film microstructure, semiconductor performance, and modeling of majority charge injection in field-effect transistors. Journal of the American Chemical Society 2004;126(42):13859–74.
[19] Newman CR, Frisbie CD, da Silva DA, Bredas JL, Ewbank PC, Mann KR. Introduction to organic thin film transistors and design of n-channel organic semiconductors. Chemistry of Materials 2004;16(23):4436–51.
[20] Murphy AR, Frechet JMJ. Organic semiconducting oligomers for use in thin film transistors. Chemical Reviews 2007;107(4):1066–96.
[21] Yoon MH, DiBenedetto SA, Russell MT, Facchetti A, Marks TJ. High-performance n-channel carbonyl-functionalized quaterthiophene semiconductors: thin-film transistor response and majority carrier type inversion via simple chemical protection/deprotection. Chemistry of Materials 2007;19(20):4864–81.
[22] Forrest SR. The path to ubiquitous and low-cost organic electronic appliances on plastic. Nature 2004;428(6986):911–8.
[23] Bracke W. Polymers with anthrazoline units in the main chain. Macromolecules 1969;2(3):286–9.
[24] Higgins J, Janovi Z. Polyanthrazolines. Journal of Polymer Science Part B: Polymer Letters 1972;10(5):357–60.
[25] Imai Y, Johnson EF, Katto T, Kurihara M, Stille JK. Synthesis of aromatic polymers containing anthrazoline and isoanthrazoline units. Journal of Polymer Science: Polymer Chemistry Edition 1975;13(10):2233–49.
[26] Stille JK. US patent, 4000187. 1976.
[27] Agrawal AK, Jenekhe SA. New conjugated polyanthrazolines containing thiophene moieties in the main chain. Macromolecules 1991;24(25):6806–8.
[28] Agrawal AK, Jenekhe SA. Synthesis and processing of heterocyclic polymers as electronic, optoelectronic, and nonlinear optical materials. 2. New series of conjugated rigid-rod polyquinolines and polyanthrazolines. Macromolecules 1993;26(5):895–905.
[29] Jenekhe S, Agrawal A. WO Patent, 9404592-A. 1993.
[30] Jenekhe SA, Osaheni JA. WO Patent, 9512628. 1995.
[31] Agrawal AK, Jenekhe SA. Electrochemical properties and electronic structures of conjugated polyquinolines and polyanthrazolines. Chemistry of Materials 1996;8(2):579–89.
[32] Hou S, Ding M, Gao LX. Synthesis and properties of polyquinolines and polyanthrazolines containing pyrrole units in the main chain. Macromolecules 2003;36(11):3826–32.
[33] Rusanov AL, Komarova LG, Prigozhina MP, Likhatchev DY. Polyquinolines and polyanthrazolines: synthesis and properties. Uspekhi Khimii 2005;74(7):739–52.
[34] Glossman-Mitnik D, Barraza-Jimenez D, Flores-Hidalgo A, Rodriguez-Valdez LM. Molecular structure and substitution effects on diphenylanthrazolines for organic semiconductors: a theoretical study. Journal of Molecular Structure: THEOCHEM 2008;863(1–3):99–104.
[35] Liu S, Jiang P, Song G, Liu R, Zhu H. Synthesis and optical properties of a series of thermally stable diphenylanthrazolines. Dyes and Pigments 2009;81(3):218–23.
[36] Frisch MJ, Trucks GW, Schlegel HB, Scuseria GE, Robb MA, Cheeseman JR, et al. Gaussian 03, revision D.01. Wallingford CT: Gaussian, Inc.; 2004.
[37] Kohn W, Sham LJ. Self-consistent equations including exchange and correlation effects. Physical Review 1965;140(4A):1133–8.
[38] Becke AD. Density-functional thermochemistry .3. The role of exact exchange. Journal of Chemical Physics 1993;98(7):5648–52.
[39] Lee CT, Yang WT, Parr RG. Development of the colle-salvetti correlation-energy formula into a functional of the electron-density. Physical Review B 1988;37(2):785–9.
[40] Osaheni JA, Jenekhe SA. Efficient blue luminescence of a conjugated polymer exciplex. Macromolecules 1994;27(3):739–42.
[41] Yang CJ, Jenekhe SA. Conjugated aromatic polyimines. 2. Synthesis, structure, and properties of new aromatic polyazomethines. Macromolecules 1995;28(4):1180–96.
[42] Hancock JM, Gifford AP, Tonzola CJ, Jenekhe SA. High-efficiency electroluminescence from new blue-emitting oligoquinolines bearing pyrenyl or triphenyl endgroups. Journal of Physical Chemistry 2007;111(18):6875–82.
[43] Promarak V, Punkvuang A, Sudyoadsuk T, Jungsuttiwong S, Saengsuwan S, Keawin T, et al. Synthesis and characterization of N-carbazole end-capped oligofluorene-thiophenes. Tetrahedron 2007;63(36):8881–90.